

Characterizing neutron-proton equilibration in nuclear reactions with sub-zeptosecond resolution

A. Jedele, A.B. McIntosh, L. Heilborn, M. Huang, M. Youngs, A. Zarrella,
E. McCleskey, and S.J. Yennello

The density dependence of the asymmetry term is currently the largest uncertainty of the nuclear equation-of-state (EoS). These constraints can be probed using multi-nucleon exchange studies between the excited projectile-like fragment (PLF*) and the excited target-like fragment (TLF*). This neutron-proton (N-Z) equilibration is governed by the contact time between the colliding nuclei and the gradient of the potential driving the equilibration. Recently, N-Z equilibration within a single dynamically produced and deformed nuclear system has been observed [1-3]. The decaying PLF* has an angular distribution indicative of decay on a timescale shorter than its rotational period. The N-Z composition was observed to depend on the decay angle and thus on the lifetime, consistent with equilibration between regions of the decaying PLF*[4-8]. We present observations that the composition of the heaviest and second heaviest fragment evolve towards each other following first-order kinetics on a zeptosecond (zs) timescale.

We analyzed data from $^{70}\text{Zn}+^{70}\text{Zn}$, $^{64}\text{Zn}+^{64}\text{Zn}$, and $^{64}\text{Ni}+^{64}\text{Ni}$ reactions at 35A MeV using the NIMROD array [3]. Events were sorted based on atomic number with charge-symmetric fragments sorted by mass. The heaviest fragment in each event was designated as **HF** and the second heaviest was designated as **LF**. To focus on N-Z equilibration in binary decays, events were required to have $Z_H \geq 12$ and $Z_L \geq 3$. A total Z cut of $Z \geq 21$ (70% of beam) and $Z \leq 32$ for all fragments was also included. Evidence that both fragments came from the PLF* comes from the velocity distribution, where the velocity of the Z_H and Z_L are centered above the center-of-mass velocity of the TLF* and PLF* (0.135 c). The decay angle (α) is the angle between the relative velocity (v_{REL}), defined as $v_H - v_L$, and the center-of-

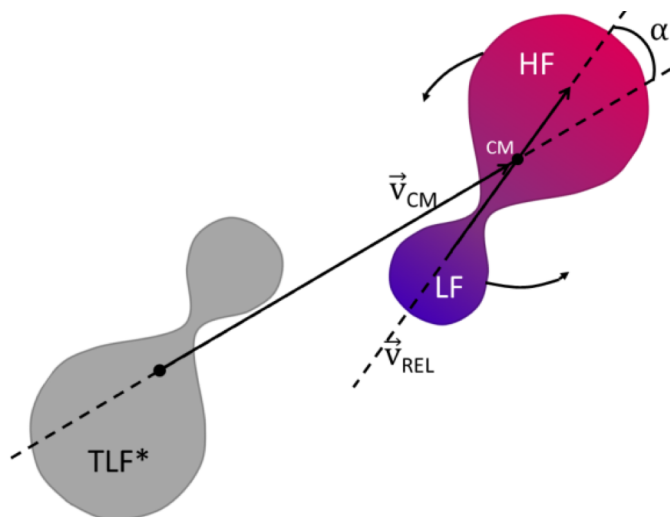


FIG. 1. Illustration of dynamical deformation and decay. The PLF* has rotated relative to the PLF*-TLF* separation axis (\vec{v}_{CM}) and is about to break up into two fragments (HF and LF). The time the PLF* lives before breaking up is measured by the angle α . The color denotes the composition with blue (red) indicating relative neutron richness (deficiency).

mass velocity (v_{CM}) of the two fragments.

The angle α was calculated using the formula

$$\alpha = \cos^{-1} \left(\frac{\vec{v}_{REL} \cdot \vec{v}_{CM}}{\|\vec{v}_{REL}\| \|\vec{v}_{CM}\|} \right).$$

Aligned emission of the Z_L in the backward direction (towards the target) corresponds to $\alpha=0^\circ$. Fig. 1 depicts α .

The angular distributions for some representative pairings of Z_H and Z_L are shown in Fig. 2. There are two distinct features present in all three pairings ($Z_H=14$, and $Z_L=5$, $Z_H=14$, and $Z_L=7$, $Z_H=12$ and $Z_L=7$). First, there is a flat distribution from $\cos(\alpha) = -1$ to $\cos(\alpha) = 0$, indicative of statistical decay. The slight increase in yield at $\cos(\alpha) = -1$ is consistent with a rotating PLF* source. Statistical decay is also evident between $\cos(\alpha) = 0$ and $\cos(\alpha) = 1$. However, the presence of a large yield peaked near $\cos(\alpha) = 1$ implies a second decay mechanism, specifically, dynamical decay. This finding is consistent with

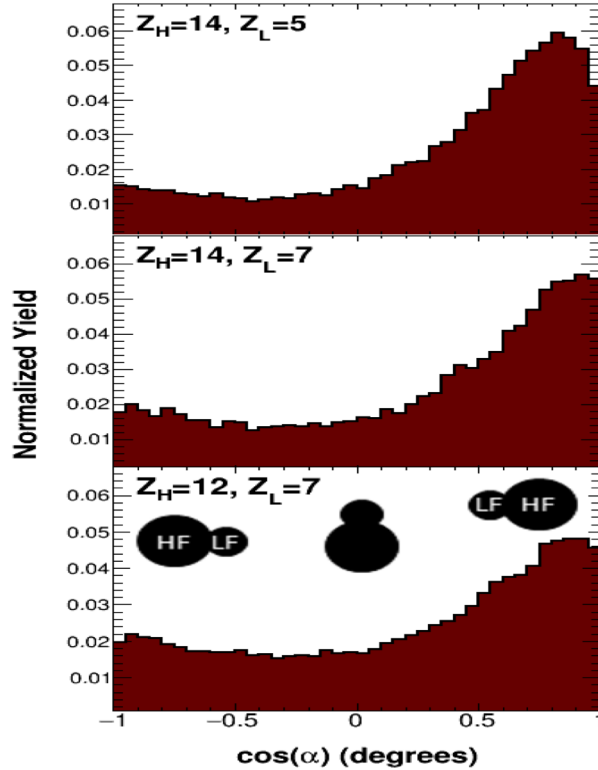


FIG. 2. Normalized angular distribution for representative Z_H and Z_L pairings. Emission of the lighter charged fragment in the backward direction (toward the target) corresponds to $\cos(\alpha)=1$.

previous studies [4]. The strong presence of this mechanism for strongly aligned decay in which Z_L is emitted in the backward direction indicates a timescale of dynamical binary splitting of the PLF* much shorter than its rotational period. As the pairings become more symmetric, the peak of the relative yield

for very strongly aligned backward decay decreases and broadens, suggesting a decrease in preference for immediate dynamical decay.

Next, the composition of **HF** and **LF** were examined as a function of angle. Fig. 3 depicts a

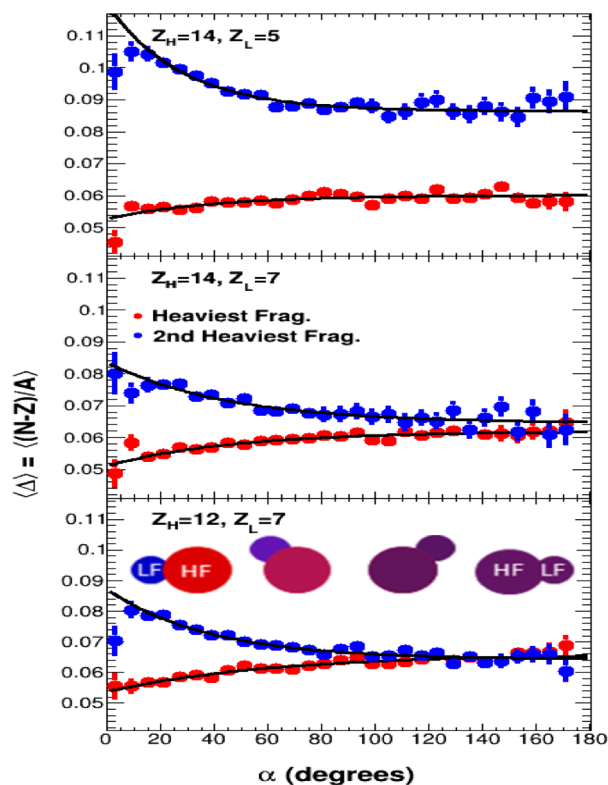


FIG. 3. Composition as a function of decay alignment showing equilibration for the same Z_H and Z_L pairings shown in Fig. 2. As the angle of rotation increases (α increases from 0°), the $\langle \Delta_L \rangle = \langle (N-L)/A \rangle$ initially decreases rapidly for Z_L and increases for Z_H before plateauing. The majority of equilibration occurs between 0° and $\sim 80^\circ$.

maximum in the $\langle \Delta_L \rangle = \langle (N-Z)/A \rangle$ for Z_L at $\alpha=0^\circ$. The composition decreases rapidly for small angles of rotation (α near 0°). As the angle increases, indicating a greater contact time, the composition levels off with most of the equilibration occurring by $\alpha=80^\circ$. A similar effect is seen in the composition of Z_H , however the composition starts off more neutron deficient. As the angle increases from 0° to 80° , the $\langle \Delta_H \rangle = \langle (N-Z)/A \rangle$ increases rapidly, followed by an leveling off by $\alpha=80^\circ$. This characteristic of the equilibration is consistent with first-order kinetics.

Results are consistent with the statistical and dynamical decay mechanisms present. Due to its dynamical deformation and the presence of a velocity gradient, the PLF* tends to break apart rapidly into two fragments along the direction of its deformation. Material close to mid-velocity corresponds to fragments emitted from the neck region, which is neutron-rich [9]. If the two fragments promptly separate, the composition of **LF** will be neutron rich and **HF** will be relatively neutron poor. As the two fragments remain in contact, their densities will evolve towards each other. The asymmetries will do likewise, resulting in more similar values of $\langle \Delta_L \rangle$ and $\langle \Delta_H \rangle$.

Given the first-order kinetics picture, all Z_H and Z_L pairings were fit with an exponential of the form: $\langle \Delta \rangle = a + be^{-c\alpha}$. The resulting fits are shown as black lines on Fig. 3. Since the angle can be related to time, the parameter c can be used as a surrogate for the rate constant. The resulting fits for all 43 pairings are consistent within statistical uncertainty. The average parameter c was 0.03 ± 0.01 per degree for Z_H and 0.02 ± 0.01 per degree for Z_L .

Next, the angle of rotation was correlated to the equilibration time through the equation:

$$t = \alpha / \omega$$

where ω is the angular frequency. The angular frequency is calculated using the equation:

$$\omega = (J\hbar) / I_{\text{eff}}$$

where J is the angular momentum and I_{eff} is the moment of inertia. The moment of inertia was calculated assuming two touching spheres **HF** and **LF** of radius r_H and r_L respectively, rotating around their common center of mass:

$$I_{\text{eff}} = m_H r_{\text{CM,H}}^2 + \frac{2}{5} m_H r_H^2 + m_L r_{\text{CM,L}}^2 + \frac{2}{5} m_L r_L^2$$

where m_H , m_L correspond to the mass of **HF** and **LF**, respectively. $r_{\text{H,CM}}$ and $r_{\text{L,CM}}$ correspond to the center-of-mass radii of the Z_H and Z_L . The angular momentum was obtained from GEMINI++ [10] simulations of the out-of-plane angular distribution of alpha particles. The width of the distribution (0.28), which is sensitive to the angular momentum, was recreated for $L=10-50\hbar$ for an excitation energy per nucleon of 0.8-1.2 MeV. The geometric mean of $22\hbar$ was used for the calculations. The resulting timescales for all pairings analyzed ranged from 2 to 4 zs with an average timescale of $3 \pm \frac{6}{1}$ zs. The average rate constant was calculated to be 3 zs^{-1} , corresponding to a mean lifetime of equilibration of 0.3 zs. These results have been submitted to Phys. Rev. Lett.

- [1] M.B. Tsang *et al.*, Phys. Rev. C **86**, 015803 (2012).
- [2] M.B. Tsang *et al.*, Phys. Rev. Lett. **92**, 062701 (2004).
- [3] Z. Kohley *et al.*, Phys. Rev. C **86**, 044605 (2012).
- [4] A.B. McIntosh *et al.*, Phys. Rev. C **81**, 034603 (2010).
- [5] S. Hudan *et al.*, Phys. Rev. C **86**, 02160 (2012).
- [6] K. Brown *et al.*, Phys. Rev. C **87**, 061601 (2013).
- [7] S. Hudan *et al.*, Eur. Phys. J. A **50**, 36 (2014).
- [8] K. Stiefel *et al.*, Phys. Rev. C **90**, 061605 (2014).